Periodic Motion Stability of a Dual-Disk Rotor System with Rub-Impact at Fixed Limiter

Qingkai Han, Zhiwei Zhang, Changli Liu, and Bangchun Wen

Abstract. The stability of periodic motions of a dual-disk rotor system, in which rub-impacts occur between a disk and a fixed limiter, is investigated. The dynamical model of the system is proposed with ordinary differential equations with two dimensional freedoms of transverse vibrations of the two rigid disks along the shaft. With the first order approximation of the piece-wisely rub-impact force, the solutions of periodic motions are deduced with harmonic expansion technique. Then, the stability and bifurcations of the system are discussed via the Floquet theory analytically. In the same range of rotating frequency, the stability analysis of the analytical solution shows good agreement with the stability and bifurcation diagrams from direct numerical integration.

Keywords: Dual-disk rotor system, rub-impact, periodic motion, stability.

1 Introduction

Unlike the traditional Jeffcott rotor model, a dual-disk rotor model is more suitable for multi-stage compressors and aero-engines when analyzing their transverse vibrations, especially when some faults exist along the shaft. Among well-known faults of a rotor system, the rub-impact between stator and rotor is a common and significant fault in many rotating machines.

As a case of vibro-impact, a mechanical system with rub-impact will behave in strong nonlinearity, e.g. the responses of the system could jump at some frequencies, and it often shows very complicated vibration phenomena, including periodic components, quasi-periodic and chaotic motions [1]. In recent decades, intensive

Qingkai Han and Bangchun Wen
School of Mechanical Engineering and Automation, Northeastern University, Shenyang 110004, China

Zhiwei Zhang
Wolfson School of Mechanical and Manufacturing Engineering, Loughborough University, Leicestershire LE11 3TU, UK

Changli Liu
School of Mechanical and Power Engineering, East China University of Science and Technology, Shanghai, 200237, China

R.A. Ibrahim et al. (Eds.): Vibro-Impact Dynamics of Ocean Systems, LNACM 44, pp. 105–119.
springerlink.com

work has been conducted on rub-impacts related dynamical phenomena in the rotor systems, partly as summarized in [2]. Based on the Jeffcott rotor system with rub-impact, Goldman and Muszynska found the supercritical subharmonic phenomenon and chaotic behavior of rotor systems [3]. The complicated behaviors of periodic, quasi-periodic and chaotic motions of them are also discussed based on the chaos and bifurcation theories in [4].

A rotor system with rub-impact can be regarded as a piecewise linear oscillator system in mathematics, where the trajectories are not smooth in its phase space due to the discontinuity of rub-impact. The typical mathematical model for rub-impact forces was introduced in a form of piecewise-linear stiffness by Beatty [5]. Many important results focusing on the periodic motion and complex dynamical behaviors of the rotor systems with rub-impacts are also documented. For example, Groll and Ewins used a numerical algorithm based on the harmonic balance method to calculate the periodic responses of a non-linear rotor/stator contact system under periodic excitation [6]. Lu gave a criterion for periodicity condition in an eccentric rotor system with analytical and numerical techniques [7]. Chu completed some experiments of rotor-to-stator full rub with various forms of periodic and chaotic vibrations [8].

In the author's previous research, periodic motions of a dual-disk rotor system with rub-impacts at fixed limiters are investigated using finite element simulations. The obtained rotor transverse vibrations with different rotating speeds, rub-impact clearances, rub-impact stiffness and rub frictions are compared with the experimental measurements [9]. It demonstrates that there are different motion patterns of the rotor system with rub-impacts, possessing periodic, dual-periodic and quasi-periodic characteristics.

In the present work, the stability of periodic motions of a dual-disk rotor system with rub-impact at a fixed limiter is investigated both analytically and numerically. The paper consists of five sections. After introduction of the research background in Section 1, a dynamical model of the rotor system with rub-impact at a fixed limiter is established in Section 2. The periodic solutions of the system are deduced in this section. In Section 3, the stability analysis of periodic motions of the system is conducted via Floquet theory. In Section 4, an example is used to demonstrate the analytical results of the periodic motions of the system compared with results from numerical simulations. Finally, some conclusions are drawn in Section 5.

2 Model Developments and Periodic Motions Analysis of the Rotor System with Rub-Impact at Fixed Limiter

2.1 Dynamical Model of the Rotor System with Rub-Impact at a Fixed Limiter

The schematic plot of the rotor system with rub-impacts is shown in Figure 1(a). The shaft rotates at an angular speed ω, and is supported by two journal bearings. There are two rigid disks mounted along the shaft. Two fixed elastic limiters are

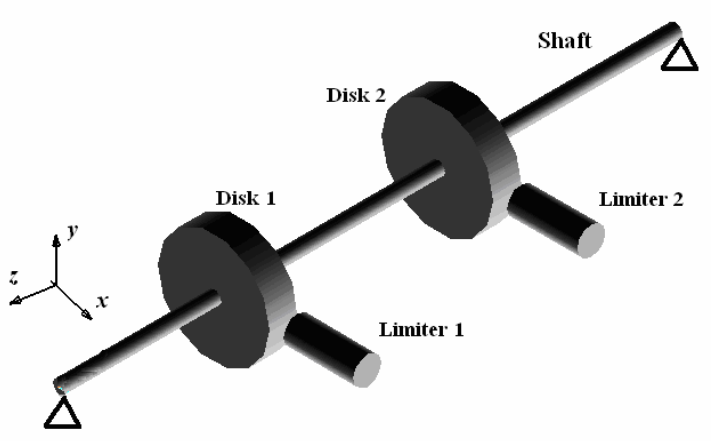

(a) Schematic plot of the dual-disk rotor system with rub-impacts at fix limiters

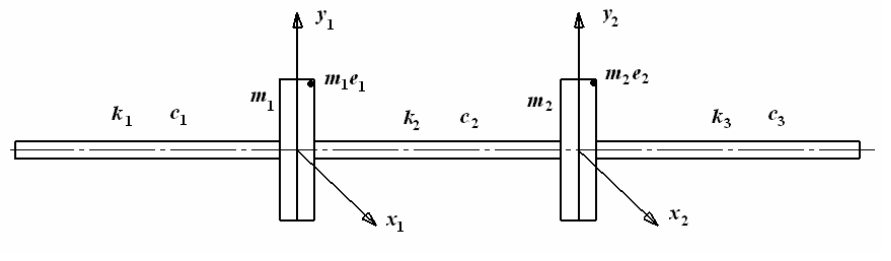

(b) Dynamical model of the rotor system

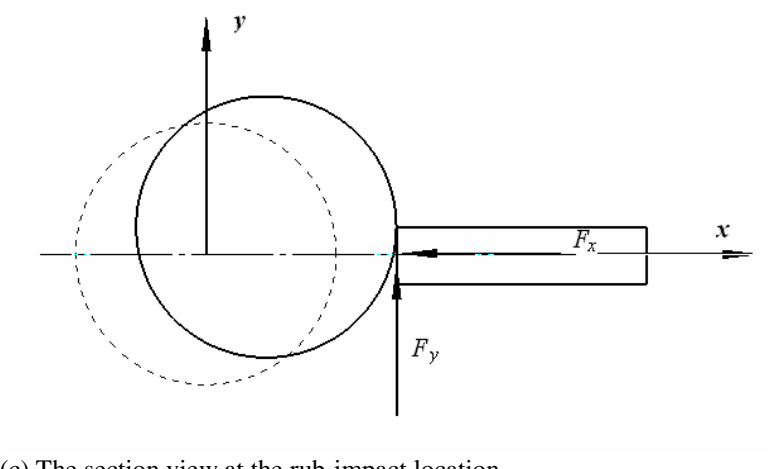

(c) The section view at the rub-impact location

Fig. 1 The dual-disk rotor system with rub-impacts at fixed limiters

mounted on the base of the test-rig. Rub-impacts can happen at one or two disks by setting the clearances between limiters and the disks.

Only transverse vibrations of the rotor system are considered. The equivalent lumped masses of the two disks are m_1, m_2. The shaft is considered as massless elastic beam. There are two unbalances at the Disk 1 and Disk 2, m_1e_1 and m_2e_2, which have the same phase. Through Figure 1(b), the differential equations of motion are written into the two groups with the total degrees of freedom (DOF) of n=4 as follows,

$$\begin{bmatrix} m_1 & 0 \\ 0 & m_2 \end{bmatrix}\begin{Bmatrix} \ddot{y}_1 \\ \ddot{y}_2 \end{Bmatrix}+\begin{bmatrix} c_{11} & c_{12} \\ c_{21} & c_{22} \end{bmatrix}\begin{Bmatrix} \dot{y}_1 \\ \dot{y}_2 \end{Bmatrix}+\begin{bmatrix} k_{11} & k_{12} \\ k_{21} & k_{22} \end{bmatrix}\begin{Bmatrix} y_1 \\ y_2 \end{Bmatrix}=\begin{Bmatrix} m_1e_1 \\ m_2e_2 \end{Bmatrix}\omega^2\sin\omega t+\begin{Bmatrix} F_{y1} \\ F_{y2} \end{Bmatrix}$$

$$\begin{bmatrix} m_1 & 0 \\ 0 & m_2 \end{bmatrix}\begin{Bmatrix} \ddot{x}_1 \\ \ddot{x}_2 \end{Bmatrix}+\begin{bmatrix} c_{11} & c_{12} \\ c_{21} & c_{22} \end{bmatrix}\begin{Bmatrix} \dot{x}_1 \\ \dot{x}_2 \end{Bmatrix}+\begin{bmatrix} k_{11} & k_{12} \\ k_{21} & k_{22} \end{bmatrix}\begin{Bmatrix} x_1 \\ x_2 \end{Bmatrix}=\begin{Bmatrix} m_1e_1 \\ m_2e_2 \end{Bmatrix}\omega^2\cos\omega t+\begin{Bmatrix} F_{x1} \\ F_{x2} \end{Bmatrix} \quad (1)$$

where $y_1, y_2, \dot{y}_1, \dot{y}_2, \ddot{y}_1, \ddot{y}_2$, $x_1, x_2, \dot{x}_1, \dot{x}_2, \ddot{x}_1, \ddot{x}_2$ are displacements, velocities and accelerations of the transverse vibrations of the two disks in y and x directions, respectively. k_{11}, k_{12}, k_{21}, k_{22} are shaft segment stiffness, which can be obtained by flexible deformations at the two disks. $c_{11}, c_{12}, c_{21}, c_{22}$ are effective damping coefficients calculated following the proportional damping assumption.

The rub-impact forces at the two disks in y and x directions of $F_{y1}, F_{y2}, F_{x1}, F_{x2}$, as shown in Figure 1(c), are

$$F_{x1}=-k_{r1}(x_1-\delta_1)H_1,\ F_{x2}=-k_{r2}(x_2-\delta_2)H_2$$
$$F_{y1}=F_{x1}f_{r1}=-k_{r1}(x_1-\delta_1)H_1f_{r1},\ F_{y2}=F_{x2}f_{r2}=-k_{r2}(x_2-\delta_2)H_2f_{r2} \quad (2)$$

where, k_{r1}, k_{r2} are the axial stiffness coefficients of the two limiters; f_{r1}, f_{r2} are the Coulomb friction coefficients at rub-impact points. δ_1, δ_2 are the initial clearances between the two limiters and disks. H_1 would be equal to 0 or 1 if $(x_1-\delta_1)$ is smaller or larger than 0, and H_2 would be equal to 0 or 1 if $(x_2-\delta_2)$ is smaller or larger than 0.

2.2 Analytical Periodic Motion Solutions of the Rotor System

Fourier expansion technique is used to derive the stable periodic solutions of the rotor system with rub-impacts. With the assumption $\theta=\omega t$, Eq (1) can be rewritten to the following differential equations as function of θ, where the differentials with respect to θ are denoted by "˙" and "′":

$$
\begin{aligned}
&y_1'' + \beta_{11} y_1' + \beta_{12} y_2' + \alpha_1 k_{11} y_1 + \alpha_1 k_{12} y_2 = e_1 \sin\theta + \alpha_1 F_{y1} \\
&y_2'' + \beta_{21} y_1' + \beta_{22} y_2' + \alpha_2 k_{21} y_1 + \alpha_2 k_{22} y_2 = e_2 \sin\theta + \alpha_2 F_{y2} \\
&x_1'' + \beta_{11} x_1' + \beta_{12} x_2' + \alpha_1 k_{11} x_1 + \alpha_1 k_{12} x_2 = e_2 \omega^2 \cos\theta + \alpha_1 F_{x1} \\
&x_2'' + \beta_{21} x_1' + \beta_{22} x_2' + \alpha_2 k_{21} x_1 + \alpha_2 k_{22} x_2 = e_2 \omega^2 \cos\theta + \alpha_2 F_{x2}
\end{aligned} \tag{3}
$$

where, $\alpha_1 = 1/(m_1\omega^2), \alpha_2 = 1/(m_2\omega^2), \beta_{11} = c_{11}/(m_1\omega)$, $\beta_{21} = c_{21}/(m_2\omega)$, $\beta_{22} = c_{22}/(m_2\omega)$.

Taking N harmonics into account, the stable periodic solutions of Eq (3) are assumed to be

$$
y_1 = a_{10} + \sum_{j=1}^{N} (a_{1j}\cos j\theta + b_{1j}\sin j\theta),\ y_2 = a_{20} + \sum_{j=1}^{N} (a_{2j}\cos j\theta + b_{2j}\sin j\theta)
$$

$$
x_1 = a_{30} + \sum_{j=1}^{N} (a_{3j}\cos j\theta + b_{3j}\sin j\theta),\ x_2 = a_{40} + \sum_{j=1}^{N} (a_{4j}\cos j\theta + b_{4j}\sin j\theta). \tag{4}
$$

In order to solve the coefficients in Eq (4), i.e. a_{10}, a_{20} , a_{30}, a_{40} , a_{1j}, b_{1j} , a_{2j}, b_{2j} , a_{3j}, b_{3j} , a_{4j}, b_{4j} , the following steps are important. Firstly, Eq (4) is substituted into Eq (3). And then all the coefficients of $\cos j\theta, \sin j\theta$ should be checked separately in different *j*-th orders. The obtained coefficients of equations are derived as follows. For the 0-th order, they are

$$
\begin{aligned}
&P_{0,1} = \frac{\alpha_1}{2\pi}\int_0^{2\pi} F_{y1} d\theta - \alpha_1 k_{11} a_{10} - \alpha_1 k_{12} a_{20} = 0, \\
&P_{0,2} = \frac{\alpha_2}{2\pi}\int_0^{2\pi} F_{y2} d\theta - \alpha_2 k_{21} a_{10} - \alpha_2 k_{22} a_{20} = 0 \\
&P_{0,3} = \frac{\alpha_1}{2\pi}\int_0^{2\pi} F_{x1} d\theta - \alpha_1 k_{11} a_{30} - \alpha_1 k_{12} a_{40} = 0, \\
&P_{0,4} = \frac{\alpha_2}{2\pi}\int_0^{2\pi} F_{x2} d\theta - \alpha_2 k_{21} a_{30} - \alpha_2 k_{22} a_{40} = 0
\end{aligned} \tag{5}
$$

For the *j*-th order, they are

$$
P_{cj,1} = j^2 a_{1j} + \frac{\alpha_1}{\pi}\int_0^{2\pi} F_{y1}\cos j\theta d\theta + \beta_{11} j b_{1j} + \beta_{12} j b_{2j} - \alpha_1 k_{11} a_{1j} - \alpha_1 k_{12} a_{2j} = 0
$$

$$
P_{cj,2} = j^2 a_{2j} + \frac{\alpha_2}{\pi}\int_0^{2\pi} F_{y2}\cos j\theta d\theta + \beta_{21} j b_{1j} + \beta_{22} j b_{2j} - \alpha_2 k_{21} a_{1j} - \alpha_2 k_{22} a_{2j} = 0
$$

$$
\begin{aligned}
P_{cj,3} = {} & j^2 a_{3j} + \frac{\alpha_1}{\pi}\int_0^{2\pi} F_{x1}\cos j\theta d\theta + \beta_{11} j b_{3j} + \beta_{12} j b_{4j} - \alpha_1 k_{11} a_{3j} - \alpha_1 k_{12} a_{4j} \\
& + e_1 N^2 \delta(j, N) = 0
\end{aligned}
$$

$$P_{cj,4} = j^2 a_{4j} + \frac{\alpha_2}{\pi}\int_0^{2\pi} F_{x2}\cos j\theta d\theta + \beta_{21} j b_{3j} + \beta_{22} j b_{4j} - \alpha_2 k_{21} a_{3j} - \alpha_2 k_{22} a_{4j}$$
$$+ e_2 N^2 \delta(j,N) = 0$$
$$P_{sj,1} = -j^2 b_{1j} + \frac{\alpha_1}{\pi}\int_0^{2\pi} F_{y1}\sin j\theta d\theta + \beta_{11} j a_{1j} + \beta_{12} j a_{2j} + \alpha_1 k_{11} b_{1j} + \alpha_1 k_{12} b_{2j}$$
$$+ e_1 N^2 \delta(j,N) = 0$$
$$P_{sj,2} = -j^2 b_{2j} + \frac{\alpha_2}{\pi}\int_0^{2\pi} F_{y2}\sin j\theta d\theta + \beta_{21} j a_{1j} + \beta_{22} j a_{2j} + \alpha_2 k_{21} b_{1j} + \alpha_2 k_{22} b_{2j}$$
$$+ e_2 N^2 \delta(j,N) = 0$$
$$P_{sj,3} = -j^2 b_{3j} + \frac{\alpha_1}{\pi}\int_0^{2\pi} F_{x1}\sin j\theta d\theta + \beta_{11} j a_{3j} + \beta_{12} j a_{4j} + \alpha_1 k_{11} b_{3j} + \alpha_1 k_{12} b_{4j} = 0$$
$$P_{sj,4} = -j^2 b_{4j} + \frac{\alpha_2}{\pi}\int_0^{2\pi} F_{x2}\sin j\theta d\theta + \beta_{12} j a_{3j} + \beta_{22} j a_{4j} + \alpha_2 k_{21} b_{3j} + \alpha_2 k_{22} b_{4j} = 0 \quad (6)$$

All these $4(N+1)$ equations are assembled into a nonlinear equation set. At last, the parameter vector of $\{a_{10}, a_{20}, a_{30}, a_{40}, a_{11}, ..., b_{4N}\}^T$ can be solved by numerical method such as the Inverse-Broyden Rank One Method.

3 Stability Analyses of Periodic Solutions of the Rotor System

3.1 Basic Theory of Floquet Stability

The stability of the fixed points of solutions of the rotor system represents the stability of its periodic motions. The original differential equations of the system, assuming that it has *n*-DOF, can be transferred into the following boundary value problem with 2*n*-DOF for the periodical solution:

$$\begin{cases} \dot{\boldsymbol{y}} = \boldsymbol{f}(t, \boldsymbol{y}) \\ \boldsymbol{f}(t+T, \boldsymbol{y}) = \boldsymbol{f}(t, \boldsymbol{y}) \\ \boldsymbol{y}(0) - \boldsymbol{y}(T) = 0 \end{cases} \quad (7)$$

Assume the periodical solution of the above Eq (7) is $\boldsymbol{y}^*(t)$. With a perturbation of $x(t) = \boldsymbol{y}(t) - \boldsymbol{y}^*(t)$ and considering the Taylor's theorem, the lowest-order term of the system retains

$$\dot{\boldsymbol{x}} = \frac{\partial \boldsymbol{f}}{\partial \boldsymbol{y}^*}\boldsymbol{x} \quad (8)$$

Equation (8) can be written as the following form with periodic coefficient matrix $\boldsymbol{A}(t)$

$$\begin{cases} \dot{\boldsymbol{x}} = \boldsymbol{A}(t)\boldsymbol{x} \\ \boldsymbol{A}(t+T) = \boldsymbol{A}(t) \end{cases} \quad (9)$$

The stability of periodical solution of $\boldsymbol{y}^*(t)$ is determined by the stability of the zero solution of Eq (9). Let $\boldsymbol{x}(0)$ be equal to $\boldsymbol{I}$, where $\boldsymbol{I}$ is the unit matrix with $2n \times 2n$ dimensions, the same as $\mathbf{A}(t)$. From Eq (9), the monodromy matrix of $\boldsymbol{S} = \boldsymbol{x}(T)$ can be obtained with numerical integration from 0 to *T*. The eigenvalues of $\boldsymbol{S}$ are the Floquet multipliers, i.e. λ_i, which are solved from $(\boldsymbol{S} - \lambda_i \boldsymbol{I})\boldsymbol{\alpha}_i = 0$. Therefore, it is possible to use the Floquet theory to discuss the stability of the periodic solutions of the rotor system.

The typical modes of Floquet multipliers leaving unit circle is plotted in Figure 2. They can be described as follows. (1) When the dominating Floquet multiplier (the eigenvalue with the largest module) lies inside the unit circle, the stable periodic solutions are asymptotically stable. (2) When the dominating Floquet multiplier lies outside of unit circle passing through (+1, 0) while the other multipliers are still inside unit circle, the stable periodic solution will lose its periodic stability and have the saddle-node bifurcation. (3) When the dominating Floquet multiplier lies outside of unit circle passing through (-1, 0) while the other multipliers are still inside unit circle, the stable periodic solution will have the period-doubling bifurcation. (4) When a pair of conjugate Floquet multipliers lies out of unit circle while other multipliers are still inside unit circle, the stable periodic solution will have the Hopf bifurcation or second Hopf bifurcation and the bifurcation will lead to an invariant torus.

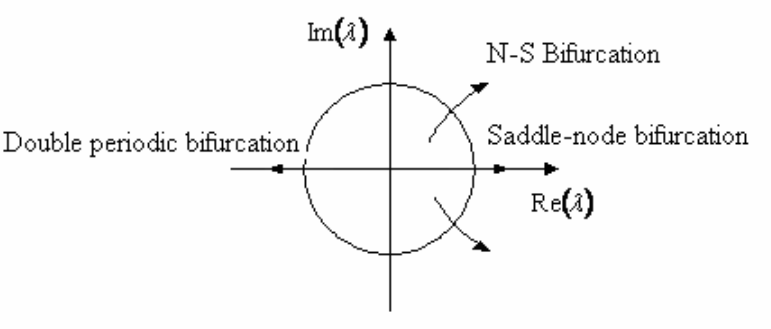

Fig. 2 Three modes of Floquet multipliers leaving unit circle

3.2 The Analytical Floquet Stability Analysis for Periodic Solutions of the Rotor System with Rub-Impact

The Floquet theory is used to discuss the stability of the obtained analytical periodic motions of the above rotor system. The dynamical equations of Eq (3) are perturbed firstly. That is, let $y_1(t) = y_{10}(t) + \Delta y_1(t)$, $y_2(t) = y_{20}(t) + \Delta y_2(t)$,

$x_1(t) = x_{10}(t) + \Delta x_1(t)$, $x_2(t) = x_{20}(t) + \Delta x_2(t)$, where $y_{10}(t)$, $y_{20}(t)$, $x_{10}(t)$, $x_{20}(t)$ are the periodic solutions obtained above. The non-linear terms of the system are also expanded into the Taylor series at the neighborhoods of stable solutions $y_{10}(t), y_{20}(t), x_{10}(t), x_{20}(t)$ and only remaining their first order terms. For Eq. (1), the obtained analytical matrix $\boldsymbol{A}(t)$ with periodic coefficients, as stated in Eq (9), is

$$\boldsymbol{A}(t)=\begin{bmatrix} 0 & 1 & 0 & 0 & 0 & 0 & 0 & 0 \\ -\alpha_1 k_{11} & -\beta_{11} & -\alpha_1 k_{12} & -\beta_{12} & \alpha_1 \dfrac{\partial F_{y1}}{\partial x_1} & 0 & 0 & 0 \\ 0 & 0 & 0 & 1 & 0 & 0 & 0 & 0 \\ -\alpha_2 k_{21} & -\beta_{21} & -\alpha_2 k_{22} & -\beta_{22} & 0 & 0 & \alpha_2 \dfrac{\partial F_{y2}}{\partial x_2} & 0 \\ 0 & 0 & 0 & 0 & 0 & 1 & 0 & 0 \\ 0 & 0 & 0 & 0 & \alpha_1(\dfrac{\partial F_{x1}}{\partial x_1} - k_{11}) & -\beta_{11} & -\alpha_1 k_{12} & -\beta_{12} \\ 0 & 0 & 0 & 0 & 0 & 0 & 0 & 1 \\ 0 & 0 & 0 & 0 & -\alpha_2 k_{21} & -\beta_{21} & \alpha_2(\dfrac{\partial F_{x2}}{\partial x_2} - k_{22}) & -\beta_{22} \end{bmatrix} \tag{10}$$

3.3 *Numerical Method for Floquet Stability Analysis for the Rotor System*

The traditional strategy of analyzing Floquet stability of a rotor system is to conduct numerical integrations based on the governing equations of the system. The commonly used method is the Runge-Kutta integration method. After the periodical responses of the rotor system are obtained with numerical integrations, i.e. the general displacement vector $\boldsymbol{y}^*$ at time T, the perturbed value of it can be approximately written as $\boldsymbol{y}^{*\prime} = (1+\Delta)\boldsymbol{y}^*$, where Δ is a small value. According to Eq. (7), the matrix of $\boldsymbol{A}(t)$ in Eq. (9) is then approximated to be

$$\boldsymbol{A}(t) = \boldsymbol{A}(t+T) \doteq \frac{\boldsymbol{f}\left(t+T, \boldsymbol{y}^*\right) - \boldsymbol{f}\left(t+T, \boldsymbol{y}^{*\prime}\right)}{\boldsymbol{y}^* - \boldsymbol{y}^{*\prime}} \tag{11}$$

With $\boldsymbol{A}(t)$ of Eq (11) and the initial value of $\boldsymbol{x}(0) = \boldsymbol{I}$, Eq (9) can be solved easily with Runge-Kutta method. Then the Floquet multipliers of the rotor system of Eq (1) are calculated as stated in Section 3.1.

4 Examples

4.1 The Model Parameters of the Rotor System

The dual-disk rotor system, as shown in Figure 1, is used to illustrate the discussions above on the stability of periodic motions. There is an unbalance on the out edge of Disk2. The rub-impact only happens at Disk 2 too. The fixed limiter is an elastic rod made of copper. The operating speeds of the shaft are between the first and the second critical speeds of the system. The parameters of the rotor system are listed in Table 1.

Table 1 Parameters of the rotor system

Parameters	Values
Shaft diameter	10mm
Shaft length	480mm
Disks' diameter	80mm
Disks' width	20mm
Density of shaft and disks	7860kg/m^3
Youg's modulus of shaft and disks	2.06e11Pa
Disks' mass	0.7902kg
Rub-impact stiffness k_rub	1e5 N/m
Rub-impact friction coefficient	0.1
Initial clearance of rub-impact	$\delta_0 = 2\text{e-}5$ m
First critical rotor speed	30.82Hz
Second critical rotor speed	119.36Hz
Shaft segement stiffness	k_{11} =2.3704e5N/m
	$k_{12} = k_{21}$ =-2.0741e5N/m
	k_{22} =2.3704e5 N/m
Damping coefficients	c_{11} =53.12N/(m/s)
	$c_{12} = c_{21}$ =-37.33 N/(m/s)
	c_{22} =53.12 N/(m/s)
Unbalance mass	1.5g at Disk 2
Unbalance radius	30mm at Disk 2
Effective unbalance distance of e2	5.695e-2mm
α_1, α_2	1.2655
β_{11}, β_{22}	67.2235
β_{12}, β_{21}	-47.2412

4.2 Analytical Solutions of the Rotor System

For the periodical motions of the rotor system with rub-impact at a fixed limiter, their first order solutions in x directions are

$$x_1 = a_{30} + a_{31}\cos\theta + b_{31}\sin\theta\,,\ x_2 = a_{40} + a_{41}\cos\theta + b_{41}\sin\theta \tag{12}$$

In order to make the integrations of Eq. (5) and (6) easier, the cubic polynomials are used to approximate the rub-impact forces at Disk 2 of F_{y2} and F_{x2}. For F_{x2}, it becomes

$$F_{x2} = p_1 x_2^3 + p_2 x_2^2 + p_3 x_2 + p_4 \tag{13}$$

For F_{y2}, it is easy to be obtained as $F_{y2} = f_{r2} F_{x2}$.

After substituting the rub-impact parameter values in Table 1, the four coefficients of Eq (13) are: p_1 = -8.026e+012, p_2 = -6.183e+008, p_3 = -8605, p_4 = 0.07482 with 95% confidence bounds.

For the system of Eq (3), with the 1st harmonic approximation of stable periodic solutions, the Equations (5) and (6) give the explicit expressions of $P_{0,1},.....,P_{sN,4}$. Nonlinear components of rub-impact forces are integrated in the interval of $[0, 2\pi]$ with respect to θ, and the coefficient equations can be written as follows,

$$\begin{aligned}
&P_{0,3} = -\alpha_1 k_{11} a_{30} - \alpha_1 k_{12} a_{40} = 0 \\
&P_{0,4} = \frac{\alpha_2}{2}(2p_1 a_{40}^3 + 3p_1 a_{41}^2 a_{40} + 3p_1 b_{41}^2 a_{40} + 2p_2 a_{40}^2 + p_2 a_{41}^2 + p_2 b_{41}^2 + 2p_3 a_{40} + 2p_4) - \\
&\alpha_2 k_{21} a_{30} - \alpha_2 k_{22} a_{40} = 0 \\
&P_{c1,3} = a_{3j} + \beta_{11} b_{3j} + \beta_{12} b_{4j} - \alpha_1 k_{11} a_{3j} - \alpha_1 k_{12} a_{4j} = 0 \\
&P_{c1,4} = a_{41} + \alpha_2(\frac{3}{4} p_1 a_{41} b_{41}^2 + 3p_1 a_{40}^2 a_{41} + 2p_2 a_{40} a_{41} + \frac{3}{4} p_1 a_{41}^3 + p_3 a_{41}) + \beta_{21} b_{31} \\
&+ \beta_{22} b_{41} - \alpha_2 k_{21} a_{31} - \alpha_2 k_{22} a_{41} + e_2 = 0 \\
&P_{s1,3} = -b_{3j} + \beta_{11} a_{31} + \beta_{12} a_{41} + \alpha_1 k_{11} b_{31} + \alpha_1 k_{12} b_{41} = 0 \\
&P_{s1,4} = -b_{41} + \alpha_2(3p_1 b_{41} a_{40}^2 + \frac{3}{4} p_1 a_{41}^2 b_{41} + 2p_2 a_{40} b_{41} + \frac{3}{4} p_1 b_{41}^3 + p_3 b_{41}) \\
&+ \beta_{21} a_{31} + \beta_{22} a_{41} + \alpha_2 k_{21} b_{31} + \alpha_2 k_{22} b_{41} = 0
\end{aligned} \tag{14}$$

Table 2 Coefficients and amplitudes of first order periodic solutions of x1 and x2

Rotating frequency	57.5 Hz	69 Hz	82 Hz
a_{30}	-3.0451e-6	-9.6994e-7	1.4114e-6
a_{31}	-5.1258e-5	-5.0808e-5	-5.7900e-5
b_{31}	-2.0418e-6	4.8913e-8	3.6793e-6
a_{40}	-3.4801e-6	-1.1085e-6	1.6130e-6
a_{41}	-3.3155e-5	-2.1993e-5	-8.6888e-6
b_{41}	-3.9047e-6	-3.9041e-6	-6.3502e-6
Amplitude of x_1 (m)	4.8239e-5	4.9838e-5	5.9428e-5
Amplitude of x_2 (m)	2.9903e-5	2.1226e-5	1.2375e-5

With Eq (14) and the parameters in Table 1, the coefficients of $a_{30}, a_{31}, b_{31}, a_{40}, a_{41}, b_{41}$ can be solved. Then the harmonic solutions of Eq (12), i.e. the periodic motions of the rotor system are obtained. The coefficients and vibration amplitudes of periodic motions under three different rotating frequencies are listed in Table 2.

4.3 *Stability Analysis of the Analytical Solutions with Floquet Theory*

Assuming that rub-impacts only occur at Disk 2, the partial differentials of rub-impact forces $\frac{\partial F_{y2}}{\partial x_2}, \frac{\partial F_{x2}}{\partial x_2}$, can be calculated based on Eq (12) and Eq (13). With the parameters in Table 1 and Table 2, Eq (9) gives

$$\boldsymbol{A}(t)=\begin{bmatrix} 0 & 1 & 0 & 0 & 0 & 0 & 0 & 0 \\ -3.00e5 & -67.22 & 2.62e5 & 47.25 & 0 & 0 & 0 & 0 \\ 0 & 0 & 0 & 1 & 0 & 0 & 0 & 0 \\ 2.62e5 & 47.25 & -3.00e5 & -67.22 & 0 & 0 & \alpha_2\frac{\partial F_{y2}}{\partial x_2} & 0 \\ 0 & 0 & 0 & 0 & 0 & 1 & 0 & 0 \\ 0 & 0 & 0 & 0 & -3.00e5 & -67.22 & 2.62e5 & 47.25 \\ 0 & 0 & 0 & 0 & 0 & 0 & 0 & 1 \\ 0 & 0 & 0 & 0 & 2.62e5 & 47.25 & \alpha_2(\frac{\partial F_{x2}}{\partial x_2}-k_{22}) & -67.22 \end{bmatrix} \tag{15}$$

where, $\frac{\partial F_{x2}}{\partial x_2} = 3p_1x_2^2 + 2p_2x_2 + p_3$, $\frac{\partial F_{y2}}{\partial x_2} = f_r(3p_1x_2^2 + 2p_2x_2 + p_3)$.

The Floquet multipliers with analytical method are calculated based on Section 3.1. On the other hand, the Floquet multipliers of the same rotor system based on the numerical integration method in Section 3.3 are also calculated. The two sets of Floquet multipliers are plotted against rotating frequency for comparison in Figure 3. It is obvious that periodic motion of the rotor system is unstable around 64Hz and 70Hz.

In addition, as shown in Figure 3, the analytical results of Floquet multipliers can not be achieved when the rotating frequency is over 72Hz. But the results with numerical integration method of $\boldsymbol{A}(t)$ can be carried on for the higher speeds. It is mainly due to the assumptions of the first order periodic solution in deducing $\boldsymbol{A}(t)$ of Eq (15).

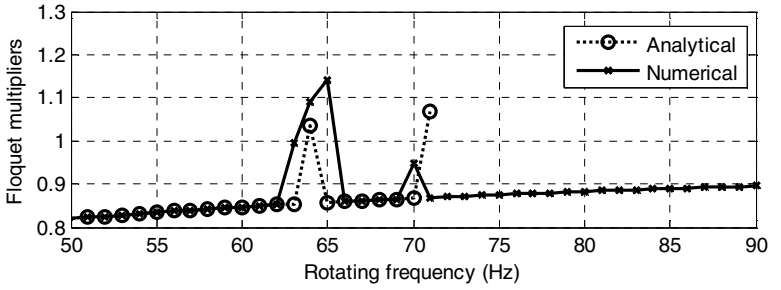

Fig. 3 Floquet multipliers vs rotating frequencies

The bifurcation charts are directly obtained with Runge-Kutta method for the rotor system of Eq (1) with parameters in Table 1. The bifurcation control parameter is the rotating speed with a range of (50, 90) Hz. As shown in Figure 4(a) and (b), when the rotating speed is less than 63Hz, the motions of the rotor system with rub-impact are stable with period 1. When rotating speed is greater than 63Hz, the system shows double periodic bifurcation. In the range from 63Hz to 70Hz of rotating speeds, the motions are in period 2 and multi-periodic. When the rotating frequency is over 70Hz, the multi-periodic motions lose their stability and the period-1 motions appear again.

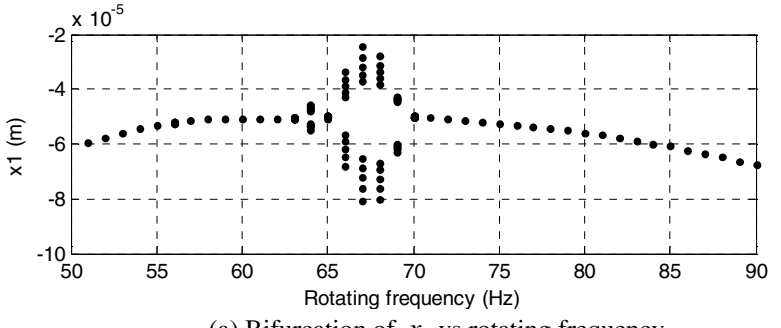

(a) Bifurcation of x_1 vs rotating frequency

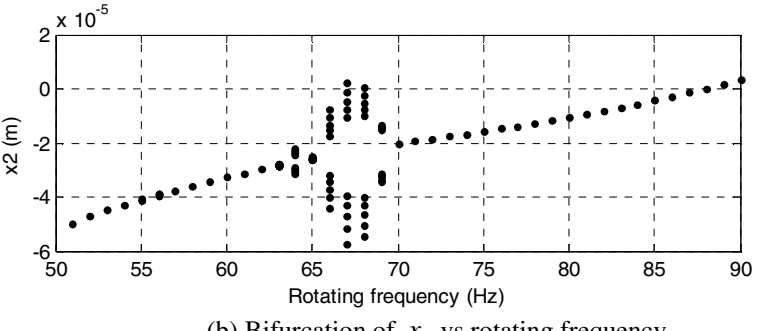

(b) Bifurcation of x_2 vs rotating frequency

Fig. 4 Bifurcations of the rotor system with rub-impact at fixed limiter

Compared with the curves in Figure 3 and 4, it can be seen that, there are many Floquet multipliers greater than 1 in the rotating frequency range of (63, 70) Hz. It means that the periodic motions tend to lose their stability in the frequency range, and meanwhile the rotor vibrations will bifurcate into double periodic motions at 63Hz. The system returns to periodic 1 after 70 Hz.

4.4 Comparisons with Numerical Integrations for Periodic Responses

The direct numerical simulations based on Runge-Kutta method are used to validate the analytical results. The numerical integrated responses of the two disks are described with transverse vibration responses and the rotor center trajectory orbits. The numerical integrated responses of the two disks with three different rotating frequencies are shown in Figure 5~7.

Figure 5 shows that rotor vibrations are periodic when rotating frequency is at 57.5Hz. The rotating frequency locates in the left region in Figure 3 and corresponds to period-1 motion.

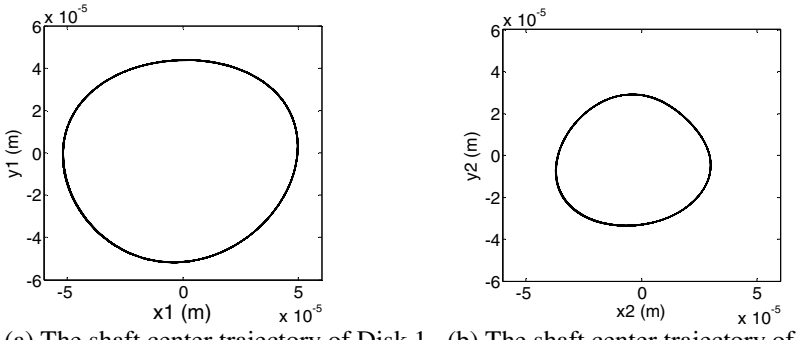

(a) The shaft center trajectory of Disk 1 (b) The shaft center trajectory of Disk 2

Fig. 5 The simulated responses of rotor system at 57.5Hz

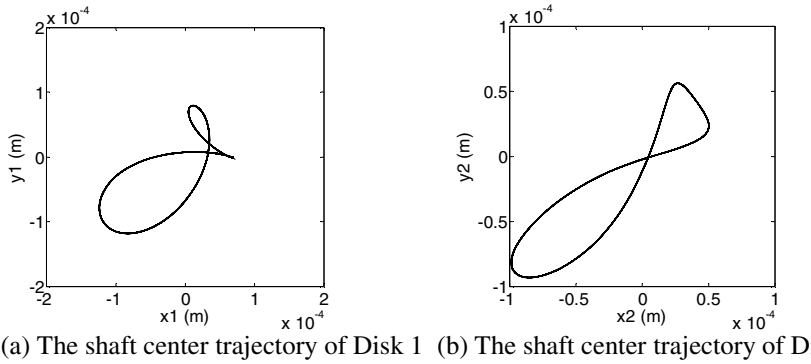

(a) The shaft center trajectory of Disk 1 (b) The shaft center trajectory of Disk 2

Fig. 6 The simulated responses of the rotor system at 69Hz

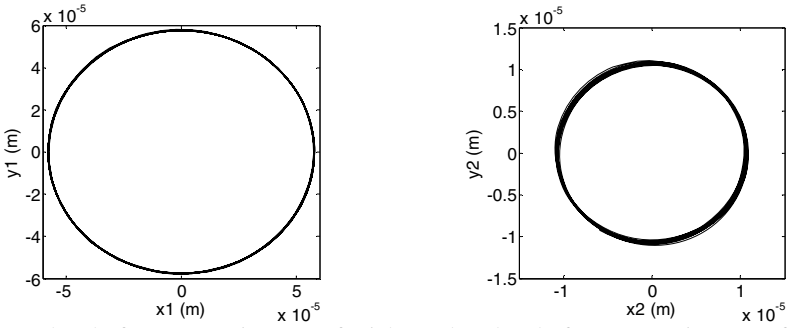

(a) The shaft center trajectory of Disk 1 (b) The shaft center trajectory of Disk 2

Fig. 7 The simulated responses of the rotor system at 82Hz

When the rotor frequency is at 69Hz, fundamental rotating frequency is disturbed by some other frequency components, as shown in Figure 6. The behavior of the shaft at 69Hz may be due to double-periodic bifurcation. This case corresponds to the middle region in Figure 3.

In Figure 7 the period-1 motion is seen again when the rotating speed is 82Hz. This case locates at the right region in Figure 3.

The simulated vibration amplitudes of the system in the above three typical cases of different rotating frequencies are listed in Table 3.

Table 3 Vibration peak-to-peak amplitudes of two disks with numerical integrations of the rotor system

Rotating freq.(Hz)	y_1 (m)	y_2 (m)	x_1 (m)	x_2 (m)
57.5	4.3929e-005	2.9221e-005	4.9751e-005	2.9959e-005
	-5.1920e-005	-3.3639e-005	-5.1944e-005	-3.7157e-05
69	7.9006e-005	5.6342e-005	6.8806e-005	5.0170e-005
	-1.1836e-004	-9.3414e-005	-1.2397e-004	-9.9102e-005
82	5.7957e-005	1.1036e-005	5.7840e-005	1.0883e-005
	-5.7941e-005	-1.1037e-005	-5.7874e-005	-1.0912e-005

5 Conclusions

The dynamical responses and their periodic motion stability analysis are carried out for a dual-disk rotor system with rub-impacts at fixed limiters.

The analytical periodic motion solutions of transverse vibrations of the rotor system due to rub-impacts at fixed limiters are deduced firstly. The motion stability is then discussed by both analytical and numerical methods based on Floquet theory. Numerical integration simulations of the rotor system are also conducted under different rotating frequencies to validate the periodical stability results.

For the presented rotor system, the stability analysis for the dual-disk rotor with rub-impact at fixed limiter indicates that there exist stable periodic motions in a large range of rotating frequency; however, in a small range of rotating frequency from 63Hz to 70Hz, the rotor system shows period-doubling bifurcations.

The analytical stability discussions for periodic motions are interesting and of great importance for understanding dual-disk rotor system with rub-impacts.

Acknowledgments. The authors gratefully acknowledge that the work was supported by Natural Science Foundation of China (Grant no. 50775028) and the 863 High-Tech Scheme (2007AA04Z418) by the Ministry of Science and Technology.

References

[1] Babitsky, V.I.: Theory of vibro-impact systems and applications. Springer, Berlin (1998)

[2] Beatty, R.: F, Differentiating rotor response due to radial rubbing, Transactions of the ASME. Journal of Vibration, Acoustics, Stress, and Reliability in Design 107, 151–160 (1995)

[3] Chu, F.: Zhang Z, Bifurcation and chaos in rub-impact Jeffcott rotor system. Journal of Sound and Vibration 210(1), 1–18 (1998)

[4] Chu, F.: Lu W, Experimental observation of nonlinear vibrations in a rub-impact rotor system. Journal of Sound and Vibration 283, 621–643 (2005)

[5] Goldman, P.: Muszynska A, Chaotic behavior of rotor/stator systems with rubs. ASME Journal of Engineering for Gas Turbine and Power 116, 692–701 (1994)

[6] von Groll, G., Ewins, D.J.: The harmonic balance method with arc-length continuation in rotor/stator contact problems. Journal of Sound and Vibration 241(2), 223–233 (2001)

[7] Muszynska, A.: Rotor-to-stationary element rub-related vibration phenomena in rotating machinery-literature survey. The Shock and Vibration Digest 21(3), 3–11 (1989)

[8] Lu, Q., Li, Q., Twizell, E.: The existence of periodic motions in rub-impact rotor systems. Journal of Sound and Vibration 264, 1127–1137 (2003)

[9] Han, Q., Zhang, Z., Wen, B.: Periodic Motions of a Dual-Disk Rotor System with Rub-Impact at Fixed Limiter, Proceedings of the Institution of Mechanical Engineers, Part C. Journal of Mechanical Engineering Science 222(C10), 1935–1946 (2008)